

AD-A111 019

RENSSELAER POLYTECHNIC INST TROY NY
HYDROGENASSISTED CRACKING IN HY-130 WELDMENTS.(U)
DEC 81 W F SAVAGE, E F NIPPES, E I HUSA

F/G 11/6

N00014-75-C-0944

NL

UNCLASSIFIED

| OF |
AD-A
711019

END
DATE
FILMED

83-82
DTIC

AD A111019

12

LEVEL II

OFFICE OF NAVAL RESEARCH

CONTRACT NO. N00014-75-C-0944, NR 031-780

FINAL

TECHNICAL REPORT

for the period

July 1, 1980 to January 31, 1981

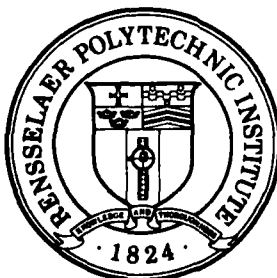
"Hydrogen-Assisted Cracking
in HY-130 Weldments"

DTIC
ELECTE
FEB 17 1982
S B

by

W.F. Savage, E.F. Nippes, and E.I. Husa

DTIC FILE COPY



DISTRIBUTION STATEMENT A

Approved for public release;
Distribution Unlimited

UNCLASSIFIED

SECURITY CLASSIFICATION OF THIS PAGE (When Data Entered)

REPORT DOCUMENTATION PAGE		READ INSTRUCTIONS BEFORE COMPLETING FORM
1. REPORT NUMBER Final Technical Report	2. GOVT ACCESSION NO. AD-A111019	3. RECIPIENT'S CATALOG NUMBER
4. TITLE (and Subtitle) HYDROGEN-ASSISTED CRACKING IN HY-130 WELDMENTS		5. TYPE OF REPORT & PERIOD COVERED Final Interim July 1, 1980-Jan. 31, 1981
		6. PERFORMING ORG. REPORT NUMBER
7. AUTHOR(s) W.F. Savage, E.F. Nippes, and E.I. Husa		8. CONTRACT OR GRANT NUMBER(s) N00014-75-C-0944, NR 031-780
9. PERFORMING ORGANIZATION NAME AND ADDRESS Rensselaer Polytechnic Institute Troy, NY 12181		10. PROGRAM ELEMENT, PROJECT, TASK AREA & WORK UNIT NUMBERS
11. CONTROLLING OFFICE NAME AND ADDRESS Procuring Contracting Officer Office of Naval Research Dept. of Navy Arlington, VA 22217		12. REPORT DATE December 23, 1981
		13. NUMBER OF PAGES
14. MONITORING AGENCY NAME & ADDRESS (if different from Controlling Office)		15. SECURITY CLASS. (of this report) Unclassified
		15a. DECLASSIFICATION/DOWNGRADING SCHEDULE
16. DISTRIBUTION STATEMENT (of this Report) REPRODUCTION OF THIS REPORT FOR ANY PURPOSE OF THE UNITED STATES GOVERNMENT		
<div style="border: 1px solid black; padding: 5px; display: inline-block;"> DISTRIBUTION STATEMENT A Approved for public release; Distribution Unlimited </div>		
17. DISTRIBUTION STATEMENT (of the abstract entered in Block 20, if different from Report)		
18. SUPPLEMENTARY NOTES		
19. KEY WORDS (Continue on reverse side if necessary and identify by block number)		
WELDING HY-130 HYDROGEN HYDROGEN-ASSISTED CRACKING EMBRITTLEMENT GMAW HYDROGEN-INDUCED CRACKING AX-140 FILLER METAL AUGMENTED STRAIN CRACKING TEST		
20. ABSTRACT (Continue on reverse side if necessary and identify by block number)		
The relative susceptibility to hydrogen-assisted cracking of AX-140 welds on HY-130 plate material and on AX-140 all-weld-metal specimens was investigated. Controlled amounts of diffusible hydrogen were introduced into these weldments by utilizing the pulsed-current gas metal arc welding (GMAW-P) process with additions of hydrogen or moisture to the shielding gas. The critical hydrogen content required for crack initiation and		

DD FORM 1473
1 JAN 73EDITION OF 1 NOV 65 IS OBSOLETE
S/N 0102-LF-014-6601

UNCLASSIFIED

SECURITY CLASSIFICATION OF THIS PAGE (When Data Entered)

UNCLASSIFIED

SECURITY CLASSIFICATION OF THIS PAGE (When Data Entered)

propagation was determined by means of the augmented strain cracking (ASC) test. Crack initiation and propagation were monitored with acoustic-emission techniques.

Although hydrogen-assisted cracking invariably initiated in the fusion zone, it frequently propagated into the heat-affected zone. Crack propagation through the weld metal was not always related to the solidification structure.

The critical hydrogen content to initiate cracking in AX-140 welds on HY-130 plate was approximately 1 ppm, whereas in AX-140 welds on AX-140 all-weld-metal the critical hydrogen content was approximately 3 ppm. This difference in cracking susceptibility was ascribed to the difference between the base-metal and the fusion-zone analyses.

The susceptibility to hydrogen-assisted cracking of all-weld-metal specimens was not sensitive to orientation, except when the ASC welding direction on a transverse section was perpendicular to the original welding direction. In this case, the critical hydrogen content was 2 ppm, rather than 3 ppm.



Accession For	
DTIC	✓
DTIC	
DTIC	
PER LETTER	
By	
Distribution/	
Availability Codes	
Avail and/or	
Dist	Special
A	

UNCLASSIFIED

TABLE OF CONTENTS

	<u>Page</u>
LIST OF TABLES	v
LIST OF FIGURES.	vi
ACKNOWLEDGEMENTS	vii
ABSTRACT	viii
INTRODUCTION	1
OBJECT	4
MATERIALS AND PROCEDURE	5
RESULTS AND DISCUSSION	23
Techniques for Adding Hydrogen to Weldments .	23
Augmented Strain Cracking Test.	32
ASC Tests of AX-140 Welds on HY-130 Steel . .	34
ASC Tests of AX-140 Welds pm AX-140 All-	
Weld Metal Specimens.	34
Comparison of Crack Susceptibility of AX-	
140 Welds	40
Combined Effect of Strain and Diffusible	
Hydrogen Content on the Crack Suscepti-	
bility.	41
Effect of Rolling Direction in HY-130	
Specimens	42
Crack Propagation	42
Acoustic Emission Studies	44
CONCLUSIONS	48
LITERATURE CITED	51

LIST OF TABLES

		<u>Page</u>
Table 1	Chemical Composition of the Materials Used in this Investigation	6
Table 2	Gas Metal Arc Welding Parameters for Producing AX-140 All-Weld-Specimens .	7
Table 3	Welding Techniques for Producing Augmented-Strain Cracking Specimens. .	13
Table 4	Diffusible Hydrogen Contents of GMA Welds, Hydrogen Added to Shielding Gas.	26
Table 5	Diffusible Hydrogen Contents of GMA-P Welds, Hydrogen Added to Shielding Gas	28
Table 6	Diffusible Hydrogen Contents of GMA-P Welds, Moisture Added to Shielding Gas	31
Table 7	Summary of Augmented-Strain-Cracking Test Results of AX-140 GMA Welds on HY-130, 30 kj/in., no preheat.	35
Table 8	Summary of Augmented-Strain-Cracking Test Results of AX-140 GMA Welds on HY-130, 30 kj/in., no preheat.	36
Table 9	Augmented-Strain-Cracking Test Results of AX-140 GMAW-P Welds on AX-140 All- Weld-Metal Specimens, 30 kj/in., no preheat.	37
Table 10	Critical Diffusible Hydrogen Content in Augmented-Strain-Cracking Tests . . .	38
Table 11	Effect of Orientation on the Augmented- Strain-Cracking Susceptibility . . .	39

LIST OF FIGURES

	<u>Page</u>
Fig. 1. Dilution of All-Weld Metal AX-140 Pad by HY-130 Base Plate	8
Fig. 2. Orientations of Augmented-Strain Cracking Test Specimens Machined from AX-140 Metal and from As-Received HY-130 Steel.	9
Fig. 3. Welding Fixture for the Preparation of ASC Test and Hydrogen Analysis Specimens.	12
Fig. 4. Low-Temperature Sawing Fixture for Sepa- rating ASC Test Specimens	14
Fig. 5. Augmented-Strain Cracking Test Fixture.	16
Fig. 6. Augmented Strain vs. Specimen Thickness in ASC Test Procedure	18
Fig. 7. Acoustic-Emission Equipment with Trans- ducer attached to ASC Test Fixture . .	19
Fig. 8. Schematic of Silicone-Oil Extraction Method for the Determination of Dif- fusible Hydrogen Content	22
Fig. 9. Diffusible Hydrogen Contents of GMAW Welds on a Metal-Added Basis, Hydrogen Additions to the Shielding Gas	25
Fig. 10. Diffusible Hydrogen Contents of GMAW-P Welds on Metal-Added Basis, Hydrogen Additions to the Shielding Gas	29
Fig. 11. Diffusible Hydrogen Contents of GMAW-P Welds on a Metal-Added Basis, Moisture Additions to the Shielding Gas	30
Fig. 12. Diffusible Hydrogen Contents of GMAW-P Welds on a Fusion-Zone Basis, Moisture Additions to the Shielding Gas	33
Fig. 13. Macrocracks Nucleated at Inclusions in HY-130. Sodium Bisulfite Etch, 50x. .	43
Fig. 14. Typical Hydrogen-Assisted Crack in ASC Specimen, 2x.	45
Fig. 15. Typical Hydrogen-Assisted Crack. Sodium- Bisulfite Etch Reveals Solidification Substructure, 40x.	46

ACKNOWLEDGEMENTS

This program was supported by the Office of Naval Research, Metallurgy and Ceramics Program, under Contract No. N00014-75-C-0944, NR 031-780. Technical monitoring of the program was provided by Dr. Bruce A. MacDonald. The authors greatly appreciate this financial and technical support.

ABSTRACT

The relative susceptibility to hydrogen-assisted cracking of AX-140 welds on HY-130 plate material and on AX-140 all-weld-metal specimens was investigated. Controlled amounts of diffusible hydrogen were introduced into these weldments by utilizing the pulsed-current gas metal arc welding (GMAW-P) process with additions of hydrogen or moisture to the shielding gas. The critical hydrogen content required for crack initiation and propagation was determined by means of the augmented strain cracking (ASC) test. Crack initiation and propagation were monitored with acoustic-emission techniques.

Although hydrogen-assisted cracking invariably initiated in the fusion zone, it frequently propagated into the heat-affected zone. Crack propagation through the weld metal was not always related to the solidification structure.

The critical hydrogen content to initiate cracking in AX-140 welds on HY-130 plate was approximately 1 ppm, whereas in AX-140 welds on AX-140 all-weld-metal the critical hydrogen content was approximately 3 ppm. This difference in cracking susceptibility was ascribed to the difference between the base-metal and the fusion-zone analyses.

The susceptibility to hydrogen-assisted cracking of all-weld-metal specimens was not sensitive to orientation, except

when the ASC welding direction on a transverse section was perpendicular to the original welding direction. In this case, the critical hydrogen content was 2 ppm, rather than 3 ppm.

INTRODUCTION

Weldments of hardenable steels are susceptible to hydrogen-induced cracking (hydrogen-assisted cracking). This cracking, which is generally transgranular, except near the initiation site, can initiate very soon after welding or after a delay period at room temperature.

Hydrogen-assisted cracking will occur only if four conditions are present simultaneously. These conditions have been identified as:¹

1. A critical concentration of diffusible hydrogen at a crack tip,
2. A stress intensity above a critical magnitude,
3. A crack-susceptible microstructure, and
4. A temperature in the range of -100 to 200°C (-150 to 400°F).

Hydrogen is introduced into weldments because the welding arc is capable of dissociating hydrogen gas, water vapor, and hydrogen-bearing compounds to produce atomic hydrogen. The molten metal will absorb atomic hydrogen in proportion to its concentration in the arc atmosphere.

In welded, high-yield strength, steel structures, the combination of service and residual stresses, ambient service temperatures, and susceptible microstructures, which are required for hydrogen-induced cracking, are inevitably present. Therefore, control of hydrogen content in these weldments is mandatory to prevent hydrogen-induced cracking.

The mechanisms proposed to explain the role of hydrogen in hydrogen-assisted cracking can be classified into four categories:

1. The creation of high internal pressure by the formation of molecular hydrogen in voids,
2. The adsorption of hydrogen on crack surfaces,
3. The reduction of binding energy by the presence of hydrogen, and
4. The modification of dislocation mobility by the presence of hydrogen.

Creation of High Internal Pressure. The "Planar Pressure Theory" proposed by Zapffe and Sims² and later modified by Tetleman³ postulates that hydrogen diffuses into the void, pressure builds to extremely high levels. The interaction of service and residual stress with this internal pressure may cause crack initiation and propagation from the initial defect sites.

Surface Adsorption. In 1952, Petch and Stables⁴ proposed a surface-adsorption theory which postulates that hydrogen adsorption at the surface of internal cracks reduces the critical fracture stress. Williams and Nelson⁵ have calculated the kinetics of crack growth based upon a surface-adsorption model and have obtained good agreement between theory and experimental results for tests conducted in gaseous hydrogen. Thus, this theory explains the effect of hydrogen on crack propagation, but it relies on dislocation pileups at grain boundaries for crack initiation.

Barth and Steiderma⁶ have criticized this theory on the basis of observations that the incubation time for crack initiation is reversible with respect to applied stress. Furthermore, the embrittlement persists at very low temperatures where both the bulk diffusion rate and the rate of redistribution of hydrogen along newly created surfaces would be negligibly small.

Reduction of Binding Energy. This theory, initially proposed by Troiano⁷, suggests that there is a stress-induced diffusion of hydrogen to positions in the lattice of high triaxial stress near a void or stress raiser. When the hydrogen concentration reaches a critical level in the triaxial-stressed region, initiation of a crack occurs. It was observed that cracking progresses discontinuously as discrete cracking events, and that cracking is preceded by an incubation period. Troiano proposes that the cohesive strength of the lattice is lowered by the presence of hydrogen in interstitial lattice sites near the crack tip.

Oriani⁸ also has proposed that the presence of hydrogen results in lattice decohesion. However, he suggested that inhomogeneity in the metal causes the intermittent cracking instead of Troiano's proposed requirement for a critical concentration of hydrogen at the crack tip of initiation and propagation of a crack.

Modification of Dislocation Mobility. Although this theory is focused upon the interaction of hydrogen with

dislocations, there have been different opinions regarding this interaction. Steinman et. al.⁹ suggest that hydrogen reduces the mobility of dislocations by restricting cross slip. This restriction might lead to large local strain concentrations which would cause crack initiation and growth. In contrast, Beachem¹⁰ proposes the pressure of hydrogen dissolved in the lattice ahead of the crack tip assists microscopic deformation processes. Thus, concentration of the hydrogen lowers the applied stress necessary to cause dislocation motion and multiplication.

OBJECT

This investigation is a study of hydrogen-assisted cracking in weldments of HY-130 steel and AX-140 all-weld-metal specimens prepared using AX-140 filler metal. This effort was performed with the following objectives:

1. To develop a method for obtaining controlled amounts of diffusible hydrogen in the weld metal utilizing the GMAW process.
2. To determine the threshold level of hydrogen required to cause cracking in HY-130/AX-140 filler metal weldments.
3. To determine the susceptibility of AX-140 weld metal to hydrogen-assisted cracking.
4. To evaluate the effect of underlying weld-metal orientation on the hydrogen-assisted crack susceptibility of all-weld-metal AX-140 material.

MATERIALS AND PROCEDURES

One heat of a 2-in. (50.8-mm) plate and one heat of AX-140 spooled filler wire were used in this study. The chemical compositions and mechanical properties of these materials are presented in Table 1. A 0.8-in. (20.3mm) thick AX-140 all-weld-metal pad was deposited on a HY-130 base plate utilizing multipass GMAW with the parameters shown in Table 2. Dilution of weld metal was characterized with the aid of an electron beam microprobe. The results, shown in Fig. 1, confirm that specimens cut from the top 0.5 in. (12.7mm) of the pad were not affected by dilution from the base metal.

Augmented Strain Cracking Test Specimens

Specimens used in the augmented strain cracking (ASC) test were machined from the all-weld-metal pad with selected orientations relative to the welding direction. Figure 2 illustrates the four orientations which were used. Additional ASC specimens were machined from the HY-130 plate with the two orientations shown at the right in Figure 2.

All ASC specimens were 2 in. (50.8mm) long by 0.5 in. (12.7mm) wide. Two thicknesses, $t=0.20$ in. (50.8mm) and $t=0.30$ in. (7.62mm), were chosen to provide small values of plastic strains in the ASC test and to permit direct comparisons with earlier work conducted at RP1.¹¹ The 2-in. (50.8mm) x 0.5-in. (12.7mm) surfaces were polished through 600-grit abrasive. Some spacer blocks 1 x 0.5 x 0.30 in.

TABLE 1
CHEMICAL COMPOSITION OF MATERIALS USED IN THIS INVESTIGATION

<u>MATERIAL</u>	<u>CONDITION</u>	<u>C</u>	<u>Mn</u>	<u>P</u>	<u>S</u>	<u>Si</u>	<u>Ni</u>	<u>Cr</u>	<u>Mo</u>	<u>V</u>	<u>Ti</u>	<u>H</u>
HY-130 HT5P2004	2" Plate	0.11	0.88	0.003	0.003	0.35	4.95	0.53	0.50	0.08	--	n.a.
AX-140 HT5L252	0.062" & 0.045" Bare Wire	0.09	1.74	0.010	0.010	0.39	2.23	1.00	0.67	0.01	0.01	1.4 ppm

MECHANICAL PROPERTIES OF MATERIALS USED

<u>MATERIAL</u>	<u>Y.S. (ksi)</u>	<u>T.S. (ksi)</u>	<u>%ELONG (2" Gage Length)</u>
HY-130 HT5P2004	134	145	21
AX-140 HT5L252	135	147	20

TABLE 2
Gas Metal Arc
Welding Parameters for
Producing AX-140 All-Weld-Metal Specimens

Electrode	AX-140
Electrode Diam.	0.063 in.
Welding Position	Flat
Transfer Mode	Spray
Polarity	DCRP
Shielding Gas	98%Ar2%O ₂
Shielding Gas Flow	45-55 CFH
Wire Feed Speed	165 ipm
Welding Current	280A
Open Circuit Voltage	30 V
Arc Voltage	26 V
Travel Speed	15 ipm
Heat Input	30 kj/in.
Contact Tube-to-Work Distance	0.75 in.
Min. Preheat and Interpass Temp.	150°F
Max. Interpass Temp.	300°F

DILUTION OF ALL-WELD-METAL
AX-140 PAD BY HY-130 BASE PLATE

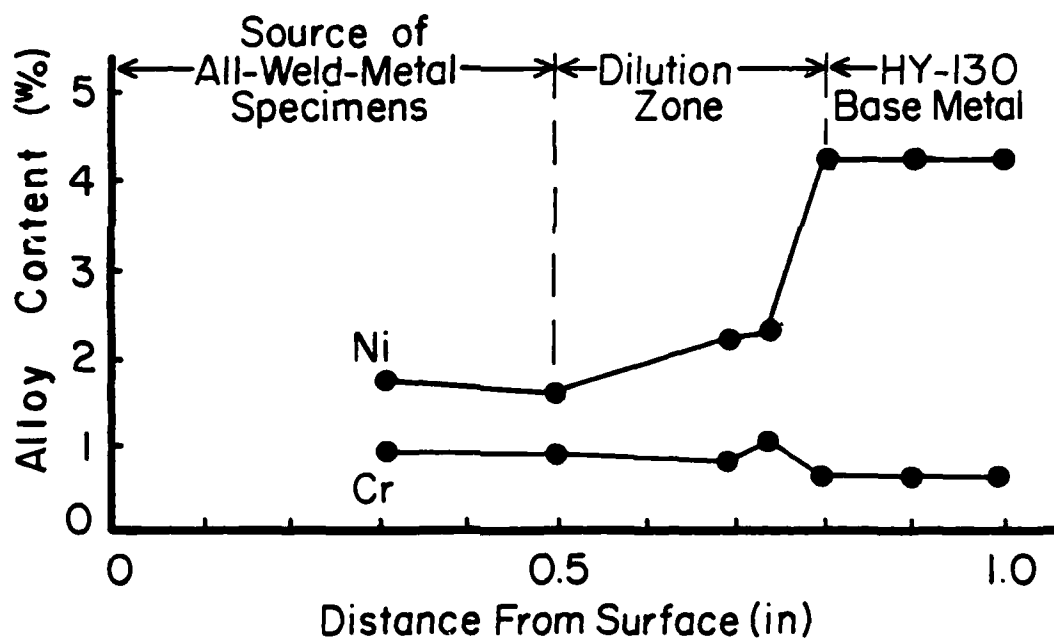
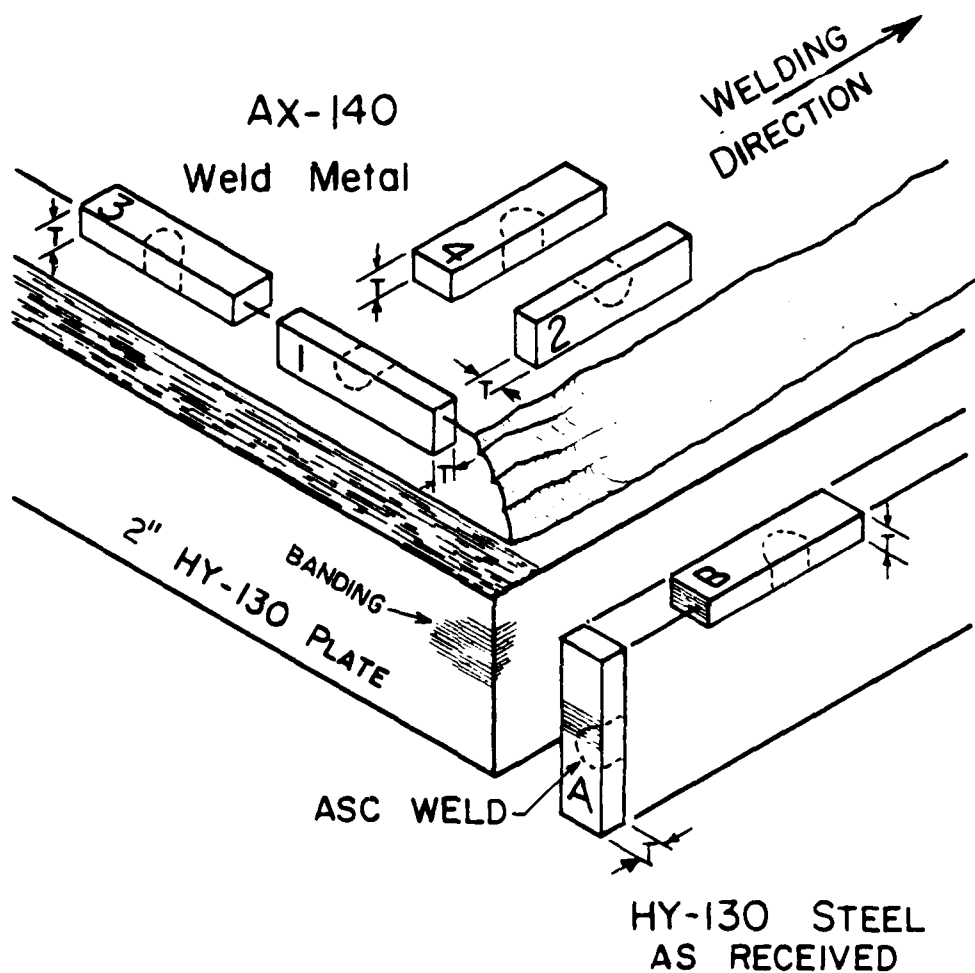


FIGURE I

Dilution of All-Weld Metal AX-140 Pad by HY-130 Base Plate

SPECIMEN ORIENTATIONS (ASC TEST)



Basic specimen dimensions
are: $2" \times 0.50" \times T$
where $T = 0.200"$ or $0.300"$

FIGURE 2

Orientations of Augmented-Strain Cracking Test Specimens
Machined from AX-140 Metal and from As-Received HY-130
Steel.

(25.4 x 12.7 x 7.62mm) were machined to size, numbered, and weighed (\pm 0.001 gm) for use either for hydrogen determination or as spacers between ASC specimens. All material, including start-up and run-off tabs, were degreased with either ethanol or acetone immediately prior to welding.

Hydrogen Content of Weld Metal

Hydrogen content of the weld metal was varied by adding either moisture or hydrogen to the shielding gas. To introduce moisture, argon-2% oxygen was bubbled through 9 in. (23 cm) of water at 24°C. This moisture-laden gas was combined with dry argon-2% oxygen gas in a mixing plenum. The moisture content of the mixture was computed from the relative flow rates. Based upon experimental measurements which showed the gas from the bubbler to be 85% saturated with moisture, the percent moisture was calculated as follows:

$$\%H_2O = \frac{(\text{CFH wet gas}) (H_2O \text{ part. press. at test temp.})}{(\text{CFH dry gas} + \text{CFH wet gas}) (\text{atmos. pres.})} \times 0.85$$

To introduce hydrogen into the shielding gas, argon - 2% oxygen was mixed with one of the following: argon -1% hydrogen, argon - 2% hydrogen, or argon -5% hydrogen. The hydrogen content of the resulting shielding gas was computed from the flow rates. In all cases, several minutes of prepurge were used to stabilize the mixtures prior to welding.

Welding and Treatment of Specimens

The ASC test specimens, spacers, and hydrogen-determination specimens were clamped in the welding fixture, with run-off tabs as shown in Fig.3. The specimens were welded using GMAW procedures recommended in shipyard specifications (Table 3, Technique S) or with pulsed -current (GMAW-P) parameters developed for easier welding with the hydrogen- or moisture-laden shielding gas (Table 3, Technique P).

Immediately after welding ,the block of specimens was unclamped and water quenched. The time interval between weld completion and quenching was approximately ten seconds. After approximately 20 seconds in the water bath, the block of specimens was transferred to a dry ice and ethanol bath at -70°C (-94°F). Subsequently, the block of specimens was taken from this bath and the hydrogen-determination specimens were separated from the ASC-spacer pairs with a hammer and a chisel. All specimens were then stored in liquid nitrogen at -196°C (-320°F) prior to hydrogen determination or separation of the ASC specimens from the spacers.

Each ASC specimen was separated from the attached spacer without significant warming by using a 0.036 in. (0.914-mm) thick slitting saw mounted in an arbor mill. Figure 4 shows the special fixture used to hold the pieces. Throughout this operation the specimen was immersed in a plastic container filled with liquid nitrogen.

The saw-cut face of the ASC specimen was repolished to

WELDING FIXTURE

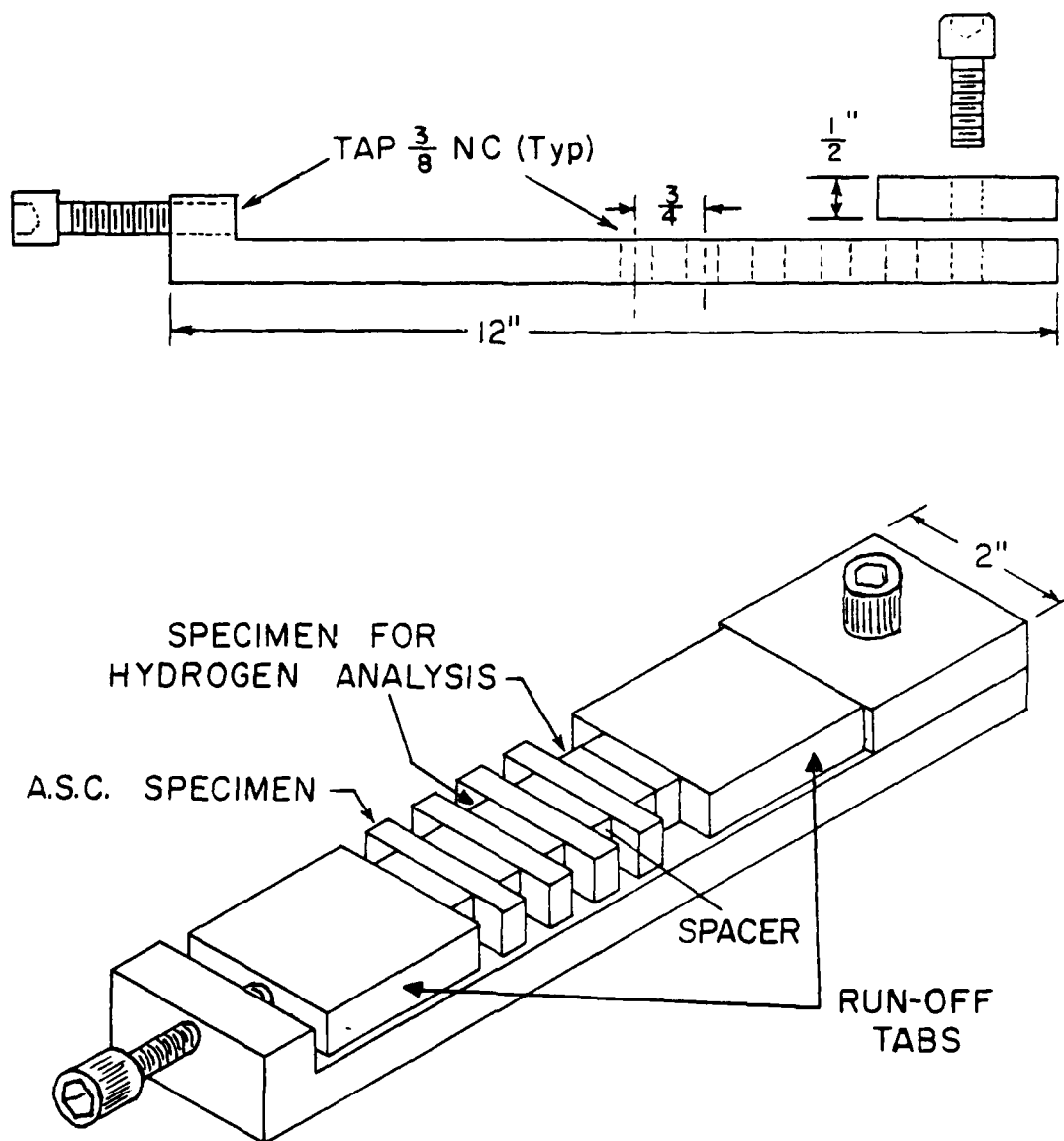


FIGURE 3

Welding Fixture for the Preparation of ASC Test and Hydrogen Analysis Specimens

TABLE 3
Welding Techniques for Producing
Augmented-Strain Cracking Specimens

	<u>Tech. S.</u>	<u>Tech. P</u>
Electrode Type	AX-140	
Electrode Diam., in.	0.063	
Welding Position	Flat	
Transfer Mode	Spray (GMAW)	Pulsed (GMAW-P)
Polarity	DCRP	DCRP 120 Hz
Shielding Gas	98%Ar2%O ₂	
Shielding Gas Flow,CFH	45-55	
Wire-Feed Speed,ipm	165	130
Welding Current, A	305	185 Avg.
Arc Voltage, V	24	29
Travel Speed, ipm	15 or 11	10.5 or 8
Heat Input, kj/in.	30 or 40	30 or 40
Contact-Tube-to-Work Distance, in.	0.375	0.94
Preheat Temp., °F	none (75°F)	
Pulse Peak Voltage, V	N/A	84
Background Current, A	N/A	34
Open-Circuit Voltage, V	30	N/A

Sawing Fixture

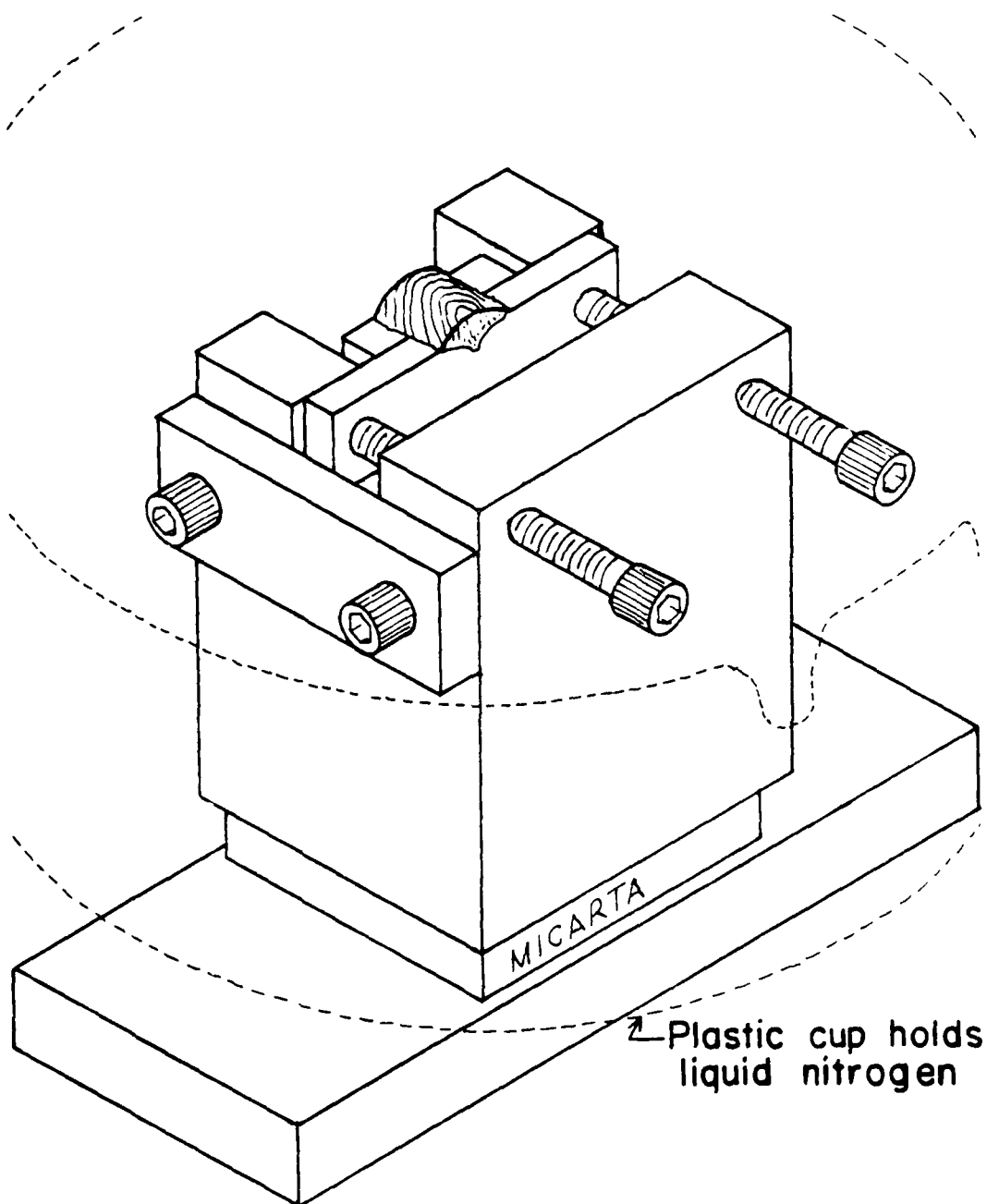


FIGURE 4

Low-Temperature Sawing Fixture for Separating ASC Test Specimens

facilitate microscopic observation of cracking during the ASC test. During repolishing, the temperature of the specimens was kept below -40°C (-40°F) by quenching in a dry ice and ethanol bath every 10 seconds to prevent hydrogen loss. A specimen holder, made from polymethylmethacrylate, was fitted with a small magnet to retain the specimen in the holder during the polishing procedure.

Augmented Strain Cracking Test

The augmented strain cracking test was designed to produce a known reproducible strain in the outer fibers of a transverse section of a weld. The critical diffusible hydrogen content required to induce cracking in a particular microstructure with a given magnitude of augmented strain can be used as an index of the susceptibility of a steel to hydrogen-assisted cracking.

Figure 5 shows the details of the fixtures used to apply strains to the ASC test specimens. The specimens were forced to conform to the surface of the radius-die block by tightening the bolt. Bending was completed before the specimen had time to warm from the liquid-nitrogen temperature, -196°C (-320°F), to the temperature range where hydrogen-assisted cracking might occur (-100 to 200°C , -150 to 400°F).

For a block with a 20-inch radius (used throughout this program) augmented strain as a function of specimen thickness was determined experimentally with the aid of electric-resistance strain gages. The approximate value of the augmented strain

Augmented Strain Cracking Fixture

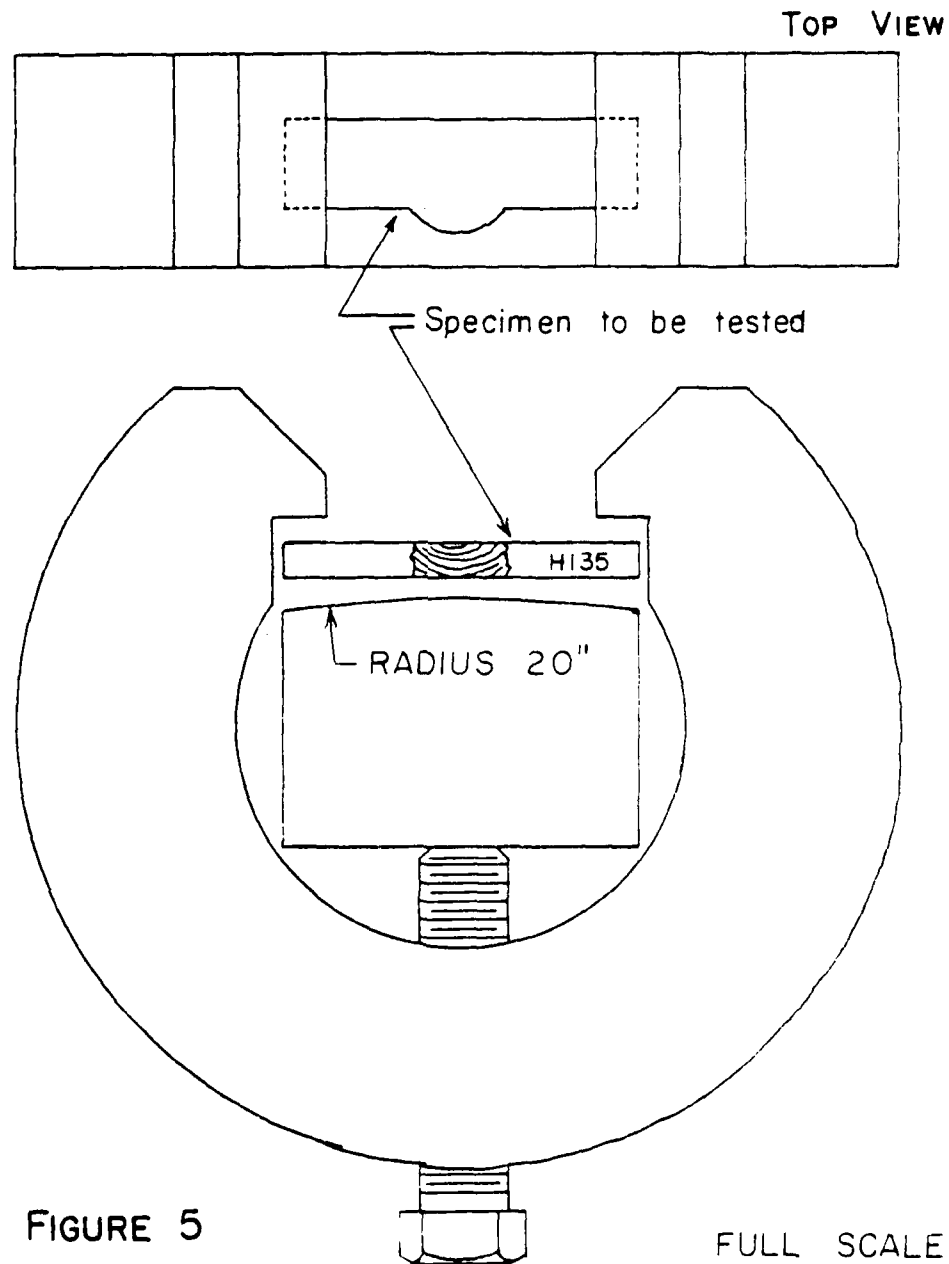


FIGURE 5

FULL SCALE

Augmented-Strain Cracking Test Fixture

determined by these tests is given by the relationship:

$$\epsilon = 1.136t/R = 0.0568t$$

where ϵ = augmented strain at the outer surface

t = thickness of ASC specimen (inches)

R = block radius = 20 inches

As may be seen in Figure 6, this relationship differs significantly from the formula derived from elastic curved-beam theory, $\epsilon = t/2R$, which is applicable to the Varestraint test¹². With the 20-inch radius die block, roughly twice the strain predicted by curved beam theory ($\epsilon = 0.025t$) is applied to ASC specimens ($\epsilon = 0.0568t$). As a result, specimen thicknesses of 0.200 in. (5.08mm) and 0.300 in. (7.62mm) produce augmented strains of approximately 1.15% and 1.70% respectively, whereas earlier investigators,^{11,13} reported 0.5% and 0.75%.

After applying the augmented strain in the test fixture, the specimen was allowed to warm to room temperature and both the initiation and growth of hydrogen-induced cracks were observed under a microscope and monitored acoustically.

Acoustic-Emission Instrumentation

To provide additional information on the initiation and propagation of hydrogen-induced cracking, the ASC testing device was instrumented to detect acoustic waves. A Model 201 Acoustic Emission Technology Corporation Signal Processor with matching preamplifier and accelerometer is shown in Figure 7. To eliminate signals arising from extraneous sources, the test fixture was mounted on a padded stand and

AUGMENTED STRAIN VS. SPECIMEN THICKNESS

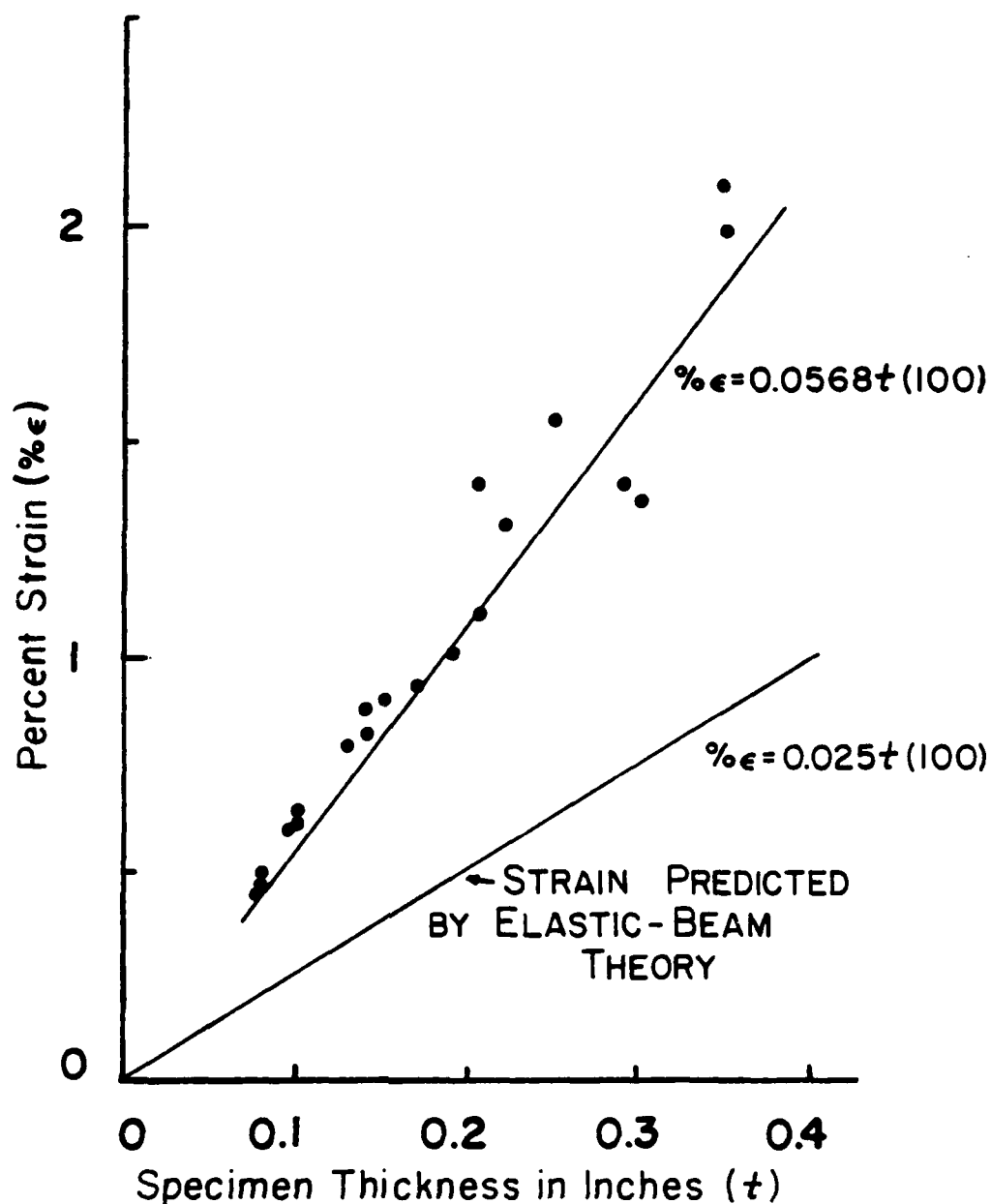


FIGURE 6

Augmented Strain vs. Specimen Thickness in ASC Test Procedure

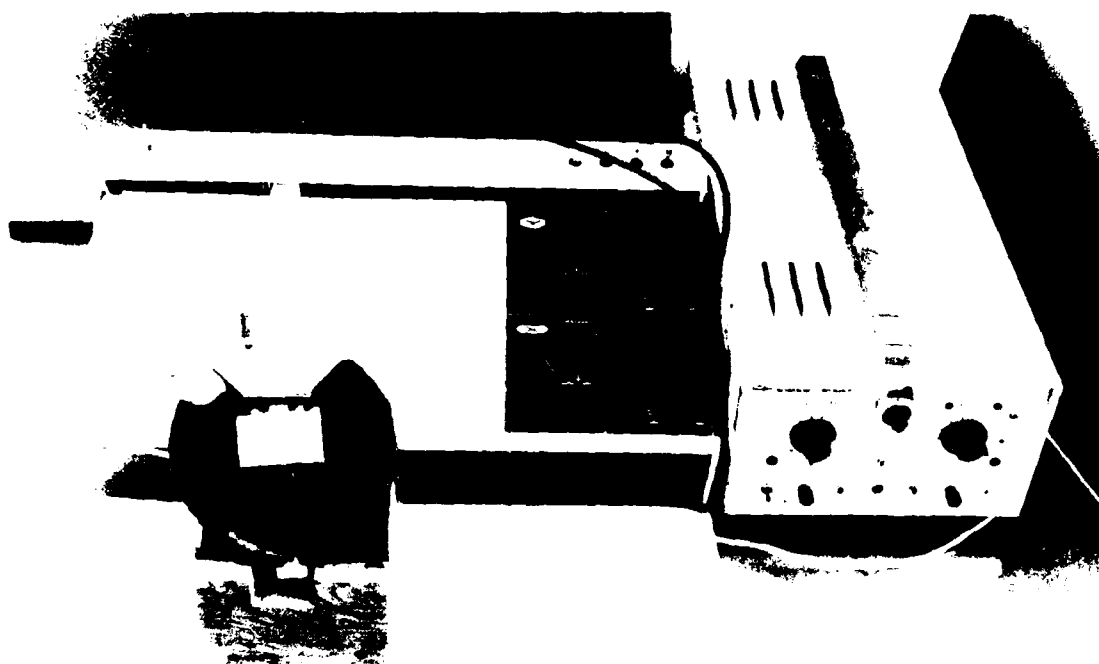


Figure 7 Acoustic-Emission Equipment with Transducer attached to ASC Test Fixture.

the accelerometer output was filtered to pass only signals with frequencies between 125 kHz and 250 kHz. The processed signals were channelled into an X-Y recorder to produce plots of total acoustic-emission counts versus time.

The acoustic-emission surveys served both for determining crack incubation time and as a means of monitoring crack growth. The incubation time for crack initiation was obtained from acoustic-emission recordings by measurement of the time delay before the first emission occurred. The summation of amplitudes of individual stress-wave emissions has been shown by Hartbower¹⁴ to be directly proportional to the crack extension as measured by a crack-opening displacement gauge. The Model 201 signal processor counts threshold level crossings and does not truly measure stress-wave amplitude. However, the underdamped transducer oscillates from a stress-wave pulse and the resulting output is roughly proportional to the stress-wave amplitude. Thus, the acoustic-emission count could be taken as a relative measure of total crack length.

Diffusible Hydrogen Analysis

The Silicone-Oil Extraction Method¹⁵, developed at RPI, was employed for determining the amount of diffusible hydrogen in the weld deposits. The evolution and volumetric measurement of the diffusible hydrogen content was accomplished by placing the welded specimen in hydrogen-saturated silicone oil at 100°C (212°F) and collecting the hydrogen liberated in a burette.

The three-step procedure for washing the specimen was

adopted from the method recommended by the BWRA:¹⁶

1. Immerse and agitate specimen in pure ethanol for 3-5 seconds.
2. Immerse and agitate in anhydrous ethyl ether for 3-5 seconds.
3. Dry with argon gas for 20-30 seconds.

The washing procedure should take no longer than 60 seconds, from liquid-nitrogen storage to placement under the funnel in the silicone-oil bath. The silicone-oil method apparatus is shown schematically in Fig. 8. Because the hydrogen extraction takes place at 100°C, the time required to complete the analysis is short, approximately 1.5 hours.

Hydrogen content on a weld-metal-added basis is computed from the relationship:

$$\text{ppm} = \frac{\Delta V}{\Delta W} \times \frac{273}{RT+273} \times \frac{AP}{760} \times 90$$

where:

ppm = diffusible hydrogen content, parts per million.

ΔV = volume of hydrogen extracted, cc.

ΔW = weight after welding minus weight before welding, gm.

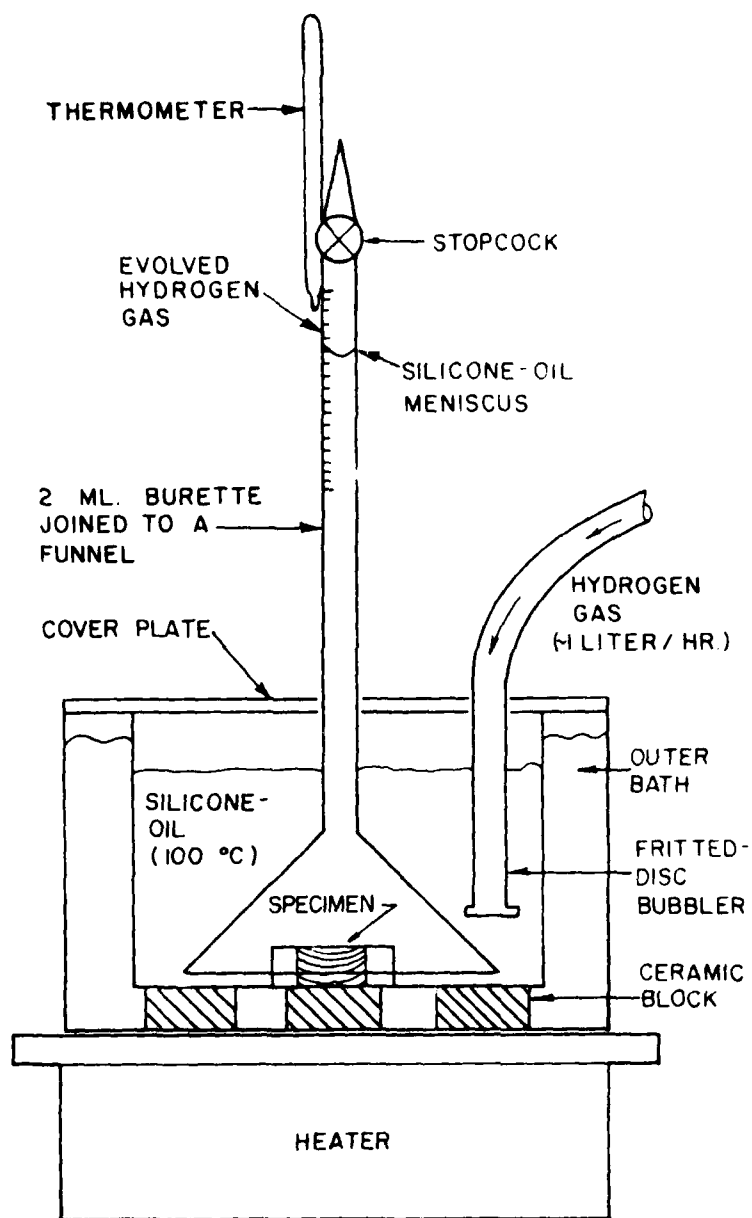
AP = atmospheric pressure, mm Hg.

RT = room temperature, °C.

90 = conversion from cc/gram to ppm.

Hydrogen content on a fused-metal basis is calculated in exactly the same way by substituting the weight of the

DETERMINATION OF DIFFUSIBLE HYDROGEN CONTENT



Silicone-Oil Extraction Method

FIGURE 8

Schematic of Silicone-Oil Extraction Method for
the Determination of Diffusible Hydrogen Content

fused metal, ΔW_F for ΔW in the above equation. The value of ΔW_F for the fused metal is calculated from the equation:

$$W_F = \frac{A_C W_F}{A_T}$$

where: A_T = cross-sectional area of specimen and weld

A_C = cross-sectional area of composite zone (fusion zone)

W_F = weight of specimen after welding, gm.

Area measurements are made with a polar planimeter on photomicrographs.

Unless otherwise stated, all values of hydrogen content were computed on a metal-added basis. To convert the hydrogen content from ppm to cc per 100gm of metal, it is necessary to multiply the former by 1.1.

RESULTS AND DISCUSSION

Techniques for Adding Hydrogen to Weldments

Hydrogen Additions to the Shielding Gas. The addition of hydrogen to the Ar-23O₂ shielding gas caused both arc instability and a decrease in arc length. Additions of 0.05 and 0.1% hydrogen caused a transition from stable spray transfer to a mixture of spray and short-circuiting transfer with considerable spatter. Hydrogen additions of 0.5% and more resulted in excessive spatter and produced irregular weld deposits with low fluidity.

For a given current and contact-tube-to work distance,

the increase in electrode stickout caused by the decrease in arc length caused an increase in the I^2R heating and, therefore, increased the melting rate. The erratic arc behavior resulted in porosity and variations in the size and shape of the weld pool, and thus caused inconsistencies in the diffusible hydrogen content of the weld metal produced by a given hydrogen addition to the shielding gas.

It was found that by increasing the current from 305 to 340 amperes and increasing the voltage from 24 to 33 volts, the spray-transfer mode could be restored and the arc behavior rendered relatively insensitive to variations in the hydrogen content of the shielding gas. However, the energy input and melting rate associated with this combination of welding variables proved to be excessive for the specimens sizes involved. Therefore, a more appropriate set of parameters involving pulsed-current (GMAW-P) was developed. These parameters are listed as Technique P in Table 3, and were found to tolerate up to 2.5% hydrogen in the shielding gas.

Figure 9 and Table 4 summarize the hydrogen contents produced by hydrogen additions to the shielding gas with continuous-current GMAW. Since, for a given hydrogen concentration in the shielding gas, the amount of hydrogen absorbed by the weld metal is directly proportional to the size of the weld pool, the relatively high scatter in these data can be attributed to the arc instability caused by adding hydrogen to the shielding gas.

DIFFUSIBLE HYDROGEN CONTENTS
GMAW Welds
Metal-Added Basis

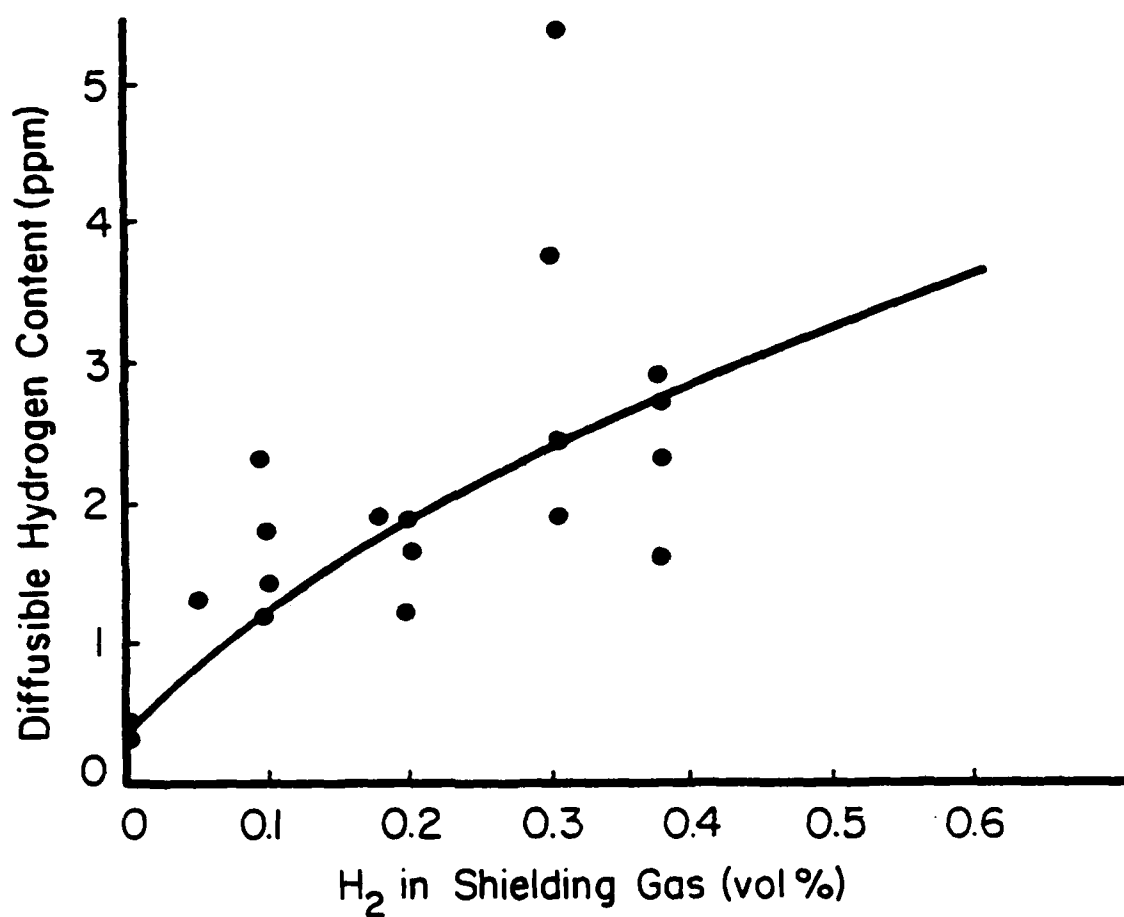


FIGURE 9

Diffusible Hydrogen Contents of GMAW Welds on a Metal-Added Basis, Hydrogen Additions to the Shielding Gas

TABLE 4
Diffusible Hydrogen Contents
of GMA Welds
Hydrogen Added to Shielding Gas

Run No.	% H ₂ O in Gas	Diffusible Hydrogen Content, ppm (metal-added basis)	
		Individual Specimens	Average
1	0.0	0.4, 0.3	0.4
2	0.05	1.3	1.3
3	0.10	1.4	1.4
4	0.10	2.3, 1.2	1.8
5	0.18	1.9	1.9
6	0.20	1.6, 1.2, 1.9	1.6
7	0.31	1.9, 3.7, 2.4	2.7
8	0.31	5.4, 3.8	4.6
9	0.38	2.3	2.3
10	0.38	2.7, 2.9, 1.6	2.4

Table 5 and Fig. 10 summarize the diffusible hydrogen contents produced by hydrogen additions to the shielding gas for pulsed GMAW. The solid lines in Figs. 9 and 10 represent the best fit of the the data for concentration of diffusible hydrogen in the weldment as a function of the hydrogen concentration in the shielding gas. The data shown in Tables 4 and 5 and Figs. 9 and 10 were calculated as ppm of hydrogen on the basis of added filler metal. As will be shown in a later portion of this report, the correlation between diffusible hydrogen content and concentration of hydrogen in the shielding gas is improved if the calculation is made on a fused-metal basis.

Moisture Additions to the Shielding Gas. It was also found possible to extend the range of diffusible hydrogen content by adding moisture to the shielding gas used with the GMAW-P process. As may be seen from Fig. 11 and Table 6, diffusible-hydrogen contents of approximately 11 ppm could be obtained in GMAW-P welds when the shielding gas was 85% saturated with moisture at 24°C. Moisture-saturated gas at 24°C has a water content of 2.95 volume percent; with 85% saturation the water content is 2.5%. By mixing argon nearly saturated with moisture with controlled amounts of dry argon-2% oxygen, it was possible to obtain deposits containing less than 11 ppm hydrogen. However, point-to-point differences in hydrogen content were still encountered.

The point-to-point variations in hydrogen in a test weld

TABLE 5
Diffusible Hydrogen Contents
of GMA-P Welds
Hydrogen Added to Shielding gas

<u>Run No.</u>	<u>% H₂ in Gas</u>	Diffusible Hydrogen Content, ppm (metal-added basis)	
		<u>Individual Specimens</u>	<u>Average</u>
1	0.1	0.1, 0.3, 0.3, 0.3, 0.5	0.3
2	0.18	0.9, 1.2, 1.1, 0.3, 0.7	0.8
3	0.5	2.4, 2.7, 3.6, 3.0	2.93
4	1.0	7.2, 7.0	7.1
5	1.7	7.4, 6.4	6.9
6	2.5	5.2	5.2

DIFFUSIBLE HYDROGEN CONTENTS
GMAW-P Welds
Metal-Added Basis

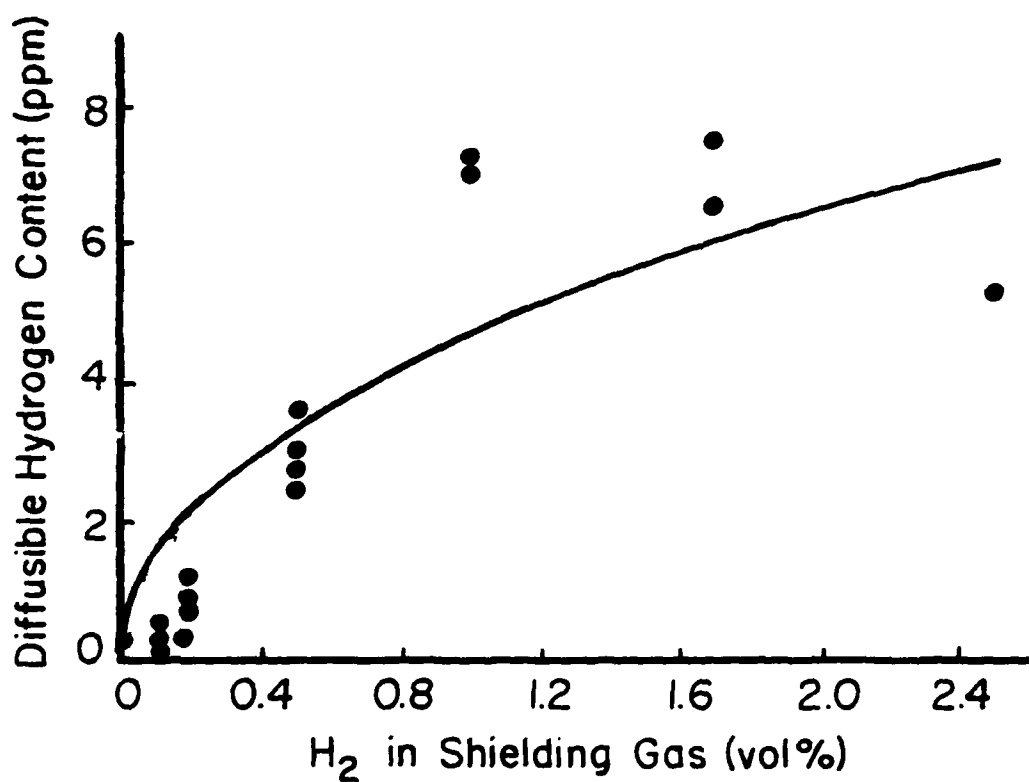


FIGURE 10

Diffusible Hydrogen Contents of GMAW-P Welds on Metal-Added Basis, Hydrogen Additions to the Shielding Gas

DIFFUSIBLE HYDROGEN CONTENTS
GMAW-P Welds
Metal-Added Basis

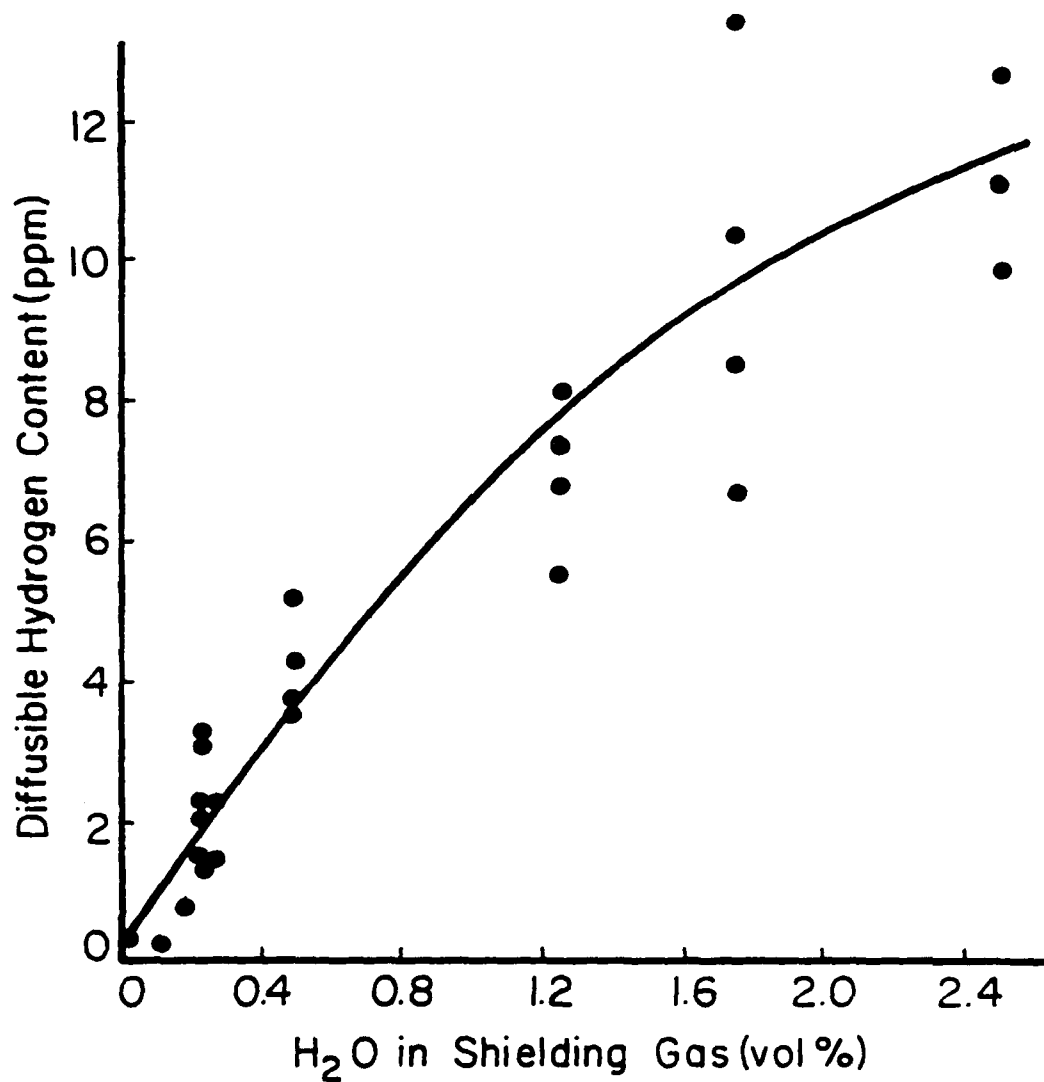


FIGURE 11

Diffusible Hydrogen Contents of GMAW-P Welds on a Metal-Added Basis, Moisture Additions to the Shielding Gas

TABLE 6
 Diffusible Hydrogen Contents
 of GMA-P Welds
 Water Added to Shielding Gas

Run No.	% H ₂ O in Gas	Diffusible Hydrogen Content, ppm (metal-added basis)	
		Individual Samples	Average
1	0.11	0.2, 0.2	0.2
2	0.18	0.72	0.72
3	0.22	1.5	1.5
4	0.22	1.5, 2.2	1.9
5	0.24	1.4, 3.3, 2.0	1.8
6	0.24	3.1, 1.3	2.2
7	0.24	2.2	2.2
8	0.50	4.3, 5.2, 3.7, 3.5	4.2
9	1.25	5.5, 6.8, 7.4, 8.1	7.4
10	1.75	13.4, 10.3, 6.7, 8.5	9.7
11	2.50	12.6, 9.8, 11.1	11.2

might have resulted from the loss of hydrogen by diffusion from the first specimens to be welded during the time when the remaining specimens were being welded. If this were the sole cause of the observed point-to-point variations, the amount of diffusible hydrogen should increase, continuously, from the beginning to the end of a test weld. However, the data from Tables 4, 5, and 6, in which the hydrogen contents of specimens within each run are listed in order of welding, do not show this trend. The scatter in the hydrogen content data was reduced significantly when the calculation of hydrogen content utilized the weight of the entire fusion zone rather than the weight of the added filler metal. Figure 12 illustrates the resultant reduction in scatter of the hydrogen-content data.

In Fig. 12, the parabolic curve is a plot, in accordance with Sieverts' Law, of the theoretical solubility of hydrogen in liquid iron at 3400°F (1870°C). The equilibrium solubility of hydrogen in iron at one atmosphere pressure, 43 ppm, at 3400°F (1871°C) was chosen so that Sieverts' Law would give a good match with the experimental data. With Sieverts' Law, the solubility of hydrogen is proportional to the square root of the volume percentage of hydrogen. In this case, because the arc dissociates water, the volume percentage of hydrogen is equal to the volume percentage of water in the shielding gas.

Augmented Strain Cracking Test

Results of augmented strain cracking (ASC) tests of AX-140

DIFFUSIBLE HYDROGEN CONTENTS
GMAW-P Welds
Fusion-Zone Basis

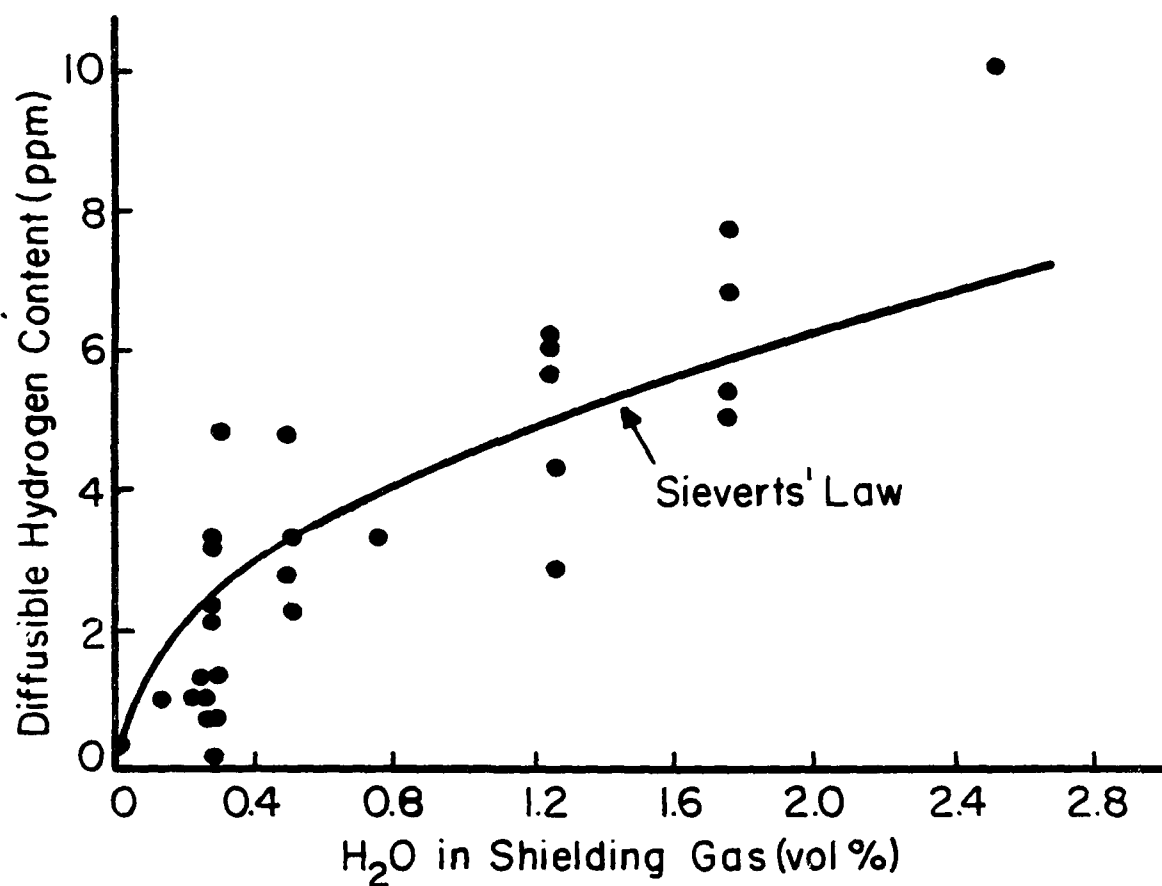


FIGURE 12

Diffusible Hydrogen Contents of GMAW-P Welds on a Fusion-Zone Basis, Moisture Additions to the Shielding Gas

GMA welds on specimens of HY-130 plate are summarized in Table 7 for 30 kj/in. and in Table 8 for 40 kj/in. The results of ASC tests of GMAW-P welds on specimens machined from the all-weld-metal pad made with AX-140 filler metal are summarized in Table 9. All welds were made using an energy input of 30 kj/in. unless otherwise noted. Cracking when it occurred, always initiated in the fusion zone of the test weld.

ASC Tests of AX-140 Welds on HY-130 Steel

The results presented in Tables 7 and 8 have been summarized in Table 10 to illustrate the critical diffusible hydrogen content at which hydrogen-assisted cracking occurred. As may be noted in Table 10, and as would be expected, for both 30 and 40 kj/in. energy input the critical hydrogen content is somewhat less for the 1.7% augmented strain than for the 1.15% augmented strain. For the same augmented strain, however, there is little difference in the critical hydrogen content of test welds made at either 30 or 40 kj/in. energy input. In summary, a diffusible hydrogen content of approximately 1 ppm is large enough to cause cracking in the ASC test when AX-140 welds are deposited on HY-130 plate with normal input and no preheat.

ASC Tests of AX-140 Welds on AX-140 All-Weld Metal Specimens

The results presented in Table 9 have been summarized in Table 11 to show the critical diffusible hydrogen content at which hydrogen-assisted cracking occurred for 1.15% augmented

TABLE 7
 Augmented Strain. Cracking Test Results
 AX-140 GMA Welds on HY-130
 30 kJ/in., No Preheat

<u>Run No.</u>	<u>Diffusible Hydrogen, ppm</u>	<u>Augmented Strain, %</u>	<u>Cracking Observed</u>	<u>Acoustic Emissions $\times 10^4$</u>	<u>Incubation Time, min.</u>
H1	0.45	1.7	No	0.1	
H2	1.1	0.75	Yes	3.6	3
		0.75	Yes	2.8	0
		1.7	Yes	5.4	0
		1.7	Yes	14.2	*
H3	1.1	1.15	No	0.4	*
		1.7	Yes	0.3	-
H4	1.7	1.7	Yes	1.0	*
H5	2.8	1.15	Yes	0.3	2
		1.7	Yes	1.0	0
H6	3.1	1.15	Yes	0.9	0
		1.15	Yes	1.6	2
		1.15	Yes	1.4	0.5
		1.15	Yes	2.0	6
H7	4.5	1.15	Yes	1.6	4
H8	4.6	1.15	Yes	0.4	*
H9	4.8	1.15	Yes	1.4	*
H10	4.8	1.7	Yes	3.1	2

* Data not available

TABLE 8

Augmented Strain Cracking Test Results

AX-140 GMA Welds on HY-130

40 kj/in., No Preheat

<u>Run No.</u>	<u>Diffusible Hydrogen, ppm</u>	<u>Augmented Strain, %</u>	<u>Cracking Observed</u>	<u>Acoustic Emissions $\times 10^4$</u>	<u>Incubation Time, min.</u>
H11	0.7	1.15	No	0.1	*
		1.7	Yes	7.4	0
H12	1.1	1.15	No	0.4	*
		1.7	No	2.1	*
		1.7	Yes	1.3	*
H13	1.9	1.15	Yes	7.8	0
		1.15	Yes	11.2	0
H14	3.0	1.15	Yes	0.9	0
		1.7	Yes	3.6	0

* Data not available

TABLE 9

Augmented-Strain-Cracking Test Results
 AX-140 GMA-P Welds on AX-140 All-Weld-Metal Specimens
 30 kj/in. No Preheat

Run No.	Orientation	Augmented Strain %	Diffusible Hydrogen Content	Cracking Observed	Acoustic Emission Count $\times 10^4$	Incubation Time, min.
A1	1	1.15	1.5 ppm	No	1.8	*
	2			No	0.2	*
	3			Yes	0.7	0
	4			No	0.4	*
A2	1	1.15	1.5	No	0.7	*
A3	1	1.7	1.5	No	0.7	*
	2			No	0.2	*
	3			No	1.6	*
	4			No	0.3	*
A4	1	1.15	2.3	No	0.1	*
	2			No	0.5	*
	3			No	0.2	*
	4			No	1.1	*
A5	1	1.15	2.8	No	0.1	*
A6	1	1.15	3.0	Yes	8.2	0
A7	1	1.15	3.3	No	0	*
	2			Yes	*	*
	3			Yes	3.0	*
	4			Yes	*	*
A8	1	1.7	3.3	Yes	3.6	3
	2			Yes	3.9	2
	3			Yes	*	10
	4			Yes	*	4
A9	1	1.7	7.0	Yes	2.8	*
	2			Yes	*	*
	3			Yes	*	*
	4			Yes	*	*

* Data not available

TABLE 10
Critical Diffusible Hydrogen Content
in Augmented-Strain Cracking Tests
AX-140 GMA Welds on HY-130
no preheat

<u>Energy Input</u> <u>kJ/in.</u>	<u>Augmented</u> <u>Strain</u> <u>%</u>	<u>Critical Diffusible</u> <u>Hydrogen Content</u> <u>ppm</u>
30	1.15	1.1 to 1.5
30	1.7	1.1
40	1.15	1.1 to 1.9
40	1.7	0.7 to 1.1

TABLE 11
Effect of Orientation on
the Augmented-Strain Cracking Susceptibility

AX-140 GMA-P Welds on
AX-140 All-Weld-Metal Specimens
30 kj/in., no preheat
Augmented Strain 1.15%

<u>Orientation</u> <u>(see Figure 2)</u>	<u>Critical Diffusible Hydrogen Content, ppm.</u>	
	<u>Fused-Metal Basis</u>	<u>Added-Metal Basis</u>
1	2 to 2.2	3.0 to 3.3
2	2.2	3.3
3	1.1 to 1.6	1.5 to 2.3
4	2.2	3.3

strain. As may be noted in Table 11 for the specimens welded with 30 kJ/in. with the GMAW-P process, only a small difference was found in the cracking susceptibility of the four different orientations of AX-140 welds on AX-140 all-weld-metal ASC specimens. Orientation 3 (Fig. 2), in which the ASC specimen was a transverse section of the all-weld-metal pad and the AX-140 weld was positioned perpendicular to the original welding direction, exhibited the greatest cracking susceptibility as evidenced by a critical hydrogen level between 1.5 and 2.3 ppm. Orientations 2 and 4, in which the ASC specimens were longitudinal sections of the all-weld-metal pad, exhibited the least cracking susceptibility, with a critical hydrogen level of 3.3 ppm. Orientation 2, in which the AX-140 test weld was positioned on the all-weld-metal pad as in a multipass weld, exhibited intermediate cracking tendencies with a critical hydrogen content between 3.0 and 3.3 ppm.

Comparison of Crack Susceptibility of AX-140 Welds

Crack susceptibility of AX-140 welds was somewhat greater when deposited on HY-130 plate material than when deposited on AX-140 weld metal. The critical hydrogen content for the former was 1.0 to 1.5 ppm, whereas the value for the latter was 3.0 to 3.3 ppm. In the case of AX-140 welds deposited on HY-130 base plate, the fused-metal zone contained approximately 30 to 35% of melted base metal. This base-metal dilution changed the composition of the fusion zone. When AX-140 welds were deposited on AX-140 all-weld-metal specimens, the composition of the fusion

zone did not change, even though 30 to 35% dilution had occurred. Obviously, the difference in composition of the weld metal accounts for the difference in cracking susceptibility. It is to be recalled that hydrogen-assisted cracking always initiated in the weld metal.

Combined Effect of Strain and Diffusible Hydrogen Content on the Crack Susceptibility

As was noted in the discussion of the ASC test results shown in Table 10, as the augmented strain was decreased from 1.7% to 1.15%, the critical diffusible hydrogen content increased. With further decrease in augmented strain, the amount of hydrogen required to cause cracking continued to increase. In one test, a specimen subjected to a strain of 0.55%, which produced a small amount of plastic deformation, experienced cracking at a diffusible hydrogen content of 4.7 ppm. With the same hydrogen content and a strain of 0.45% cracking did not occur. This strain of 0.45% is elastically equivalent to a stress of 135,000 psi, the approximate yield strength of the HY-130 plate and the AX-140 weld metal.

In an ASC test performed with 1.15% strain and a hydrogen content of 9ppm, the augmented strain was removed soon after cracking activity had been detected by acoustic emission. The ASC specimen, immediately examined at 10X magnification, exhibited no cracks. However, within two minutes after unloading, a 0.30-inch (7.5 mm) long crack grew across the face of the unloaded, but slightly plastically deformed, specimen. This

was dramatic evidence that the residual stress, which resulted from the small plastic strain during the ASC test, was ample for crack propagation when sufficient hydrogen was present.

Effect of Rolling Direction in HY-130 Specimens

Welded ASC specimens machined from HY-130 plate with the long axes perpendicular to the rolled surface (Fig. 2, Orientation A) experienced microcracking in the absence of diffusible hydrogen with only 1.15% augmented strain. In addition, acoustic emissions during ASC tests were detected in unwelded specimens machined with this orientation. The high crack susceptibility of this orientation in the HY-130 steel is attributed to the presence of elongated inclusions which were oriented with their long axes perpendicular to the stress direction. With the application of stress, these inclusions delaminated and acted as crack-initiation sites. Figure 13, at 50x magnification, shows the cracking associated with these elongated inclusions, which are located in alloy-rich bands and are orientated parallel to the rolled surface. It should be noted that a rumpled surface is present in front of the crack tips. This high crack susceptibility, associated with inclusions, prevented study of hydrogen-assisted cracking for specimens machined with this orientation. Therefore, Orientation B (Fig. 2), in which the long axis of the specimen is parallel to the rolled surface, was chosen for ASC tests of specimens machined from HY-130 plate.

Crack Propagation

Hydrogen-assisted cracks in ASC specimens were usually

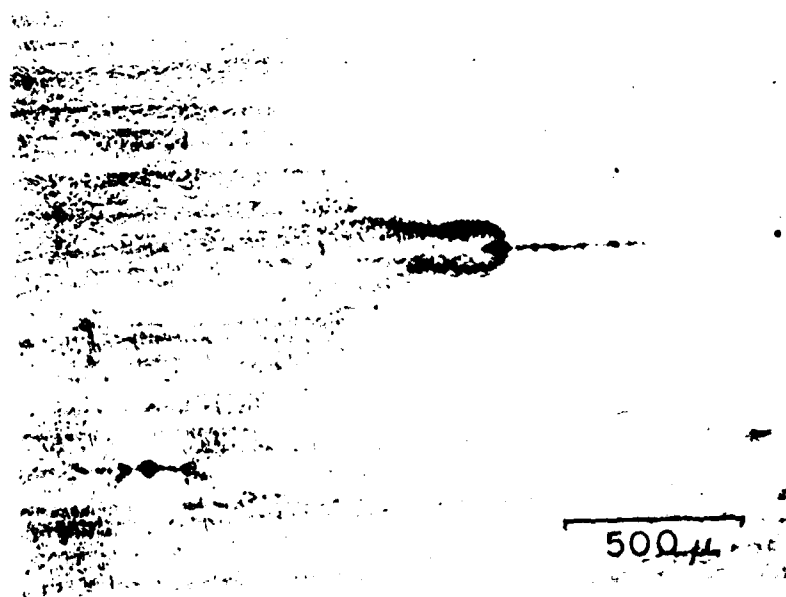
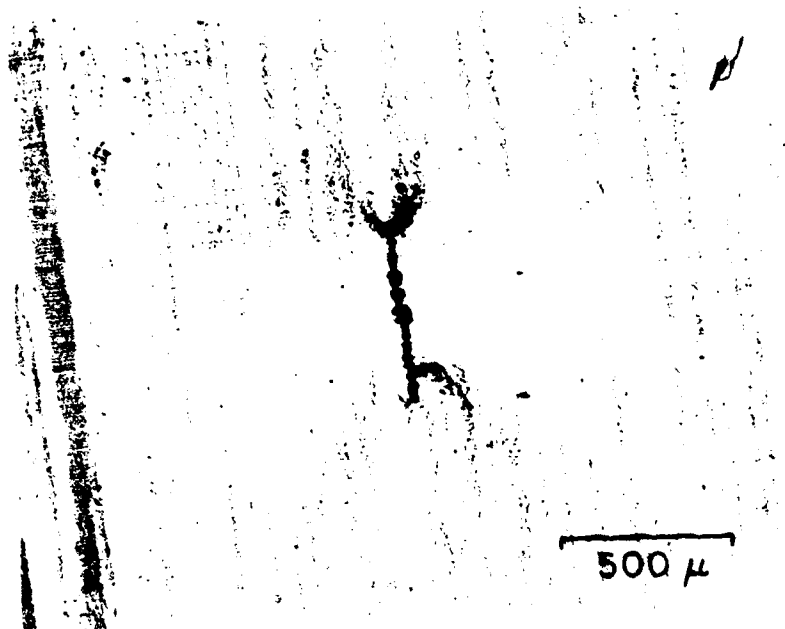


Figure 13. Micrograph of the dark structure in the center of the field of view in Figure 12, at 100X magnification.

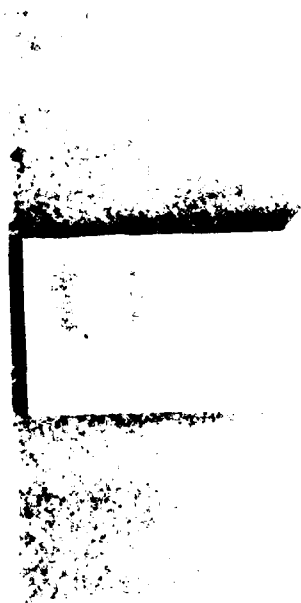
oriented normal to the principal strain, as shown in Fig. 14 at 2X. Cracking was usually observed at or near the surface of the weld. No cracks were observed to have initiated in the partially melted zone or the heat-affected zone in any of the ASC tests.

The solidification substructure and crack morphology in a typical ASC all-weld-metal specimen are shown in Fig. 15 at 40X magnification. Cracking propagated along cell boundaries only when the cells were oriented normal to the augmented strain. These regions usually exhibited the greatest crack width and are believed to have been the crack-initiation sites. Wherever the crack encountered cellular dendrite boundaries at an angle, the crack propagated in a mixed mode, partially along the boundaries and partially transverse to the subgrains.

As can be seen in Fig. 15, cracks extended into regions where the solidification substructure had been formed by previous welds. These cracks propagated in a mixed mode, partially along the boundaries and partially transverse to the subgrain. For the four orientations studied (Orientations 1-4, Fig. 2) crack propagation into the heat-affected zone did not follow a preferred orientation with respect to the original welding direction of the all-weld-metal pad.

Acoustic Emission Studies

The acoustic-emission monitoring apparatus permitted study of the crack initiation and propagation behavior during the ASC tests. As described in the procedures section, an approximate sum of stress-wave amplitudes was recorded as a function of time



1912

Photo of [illegible]

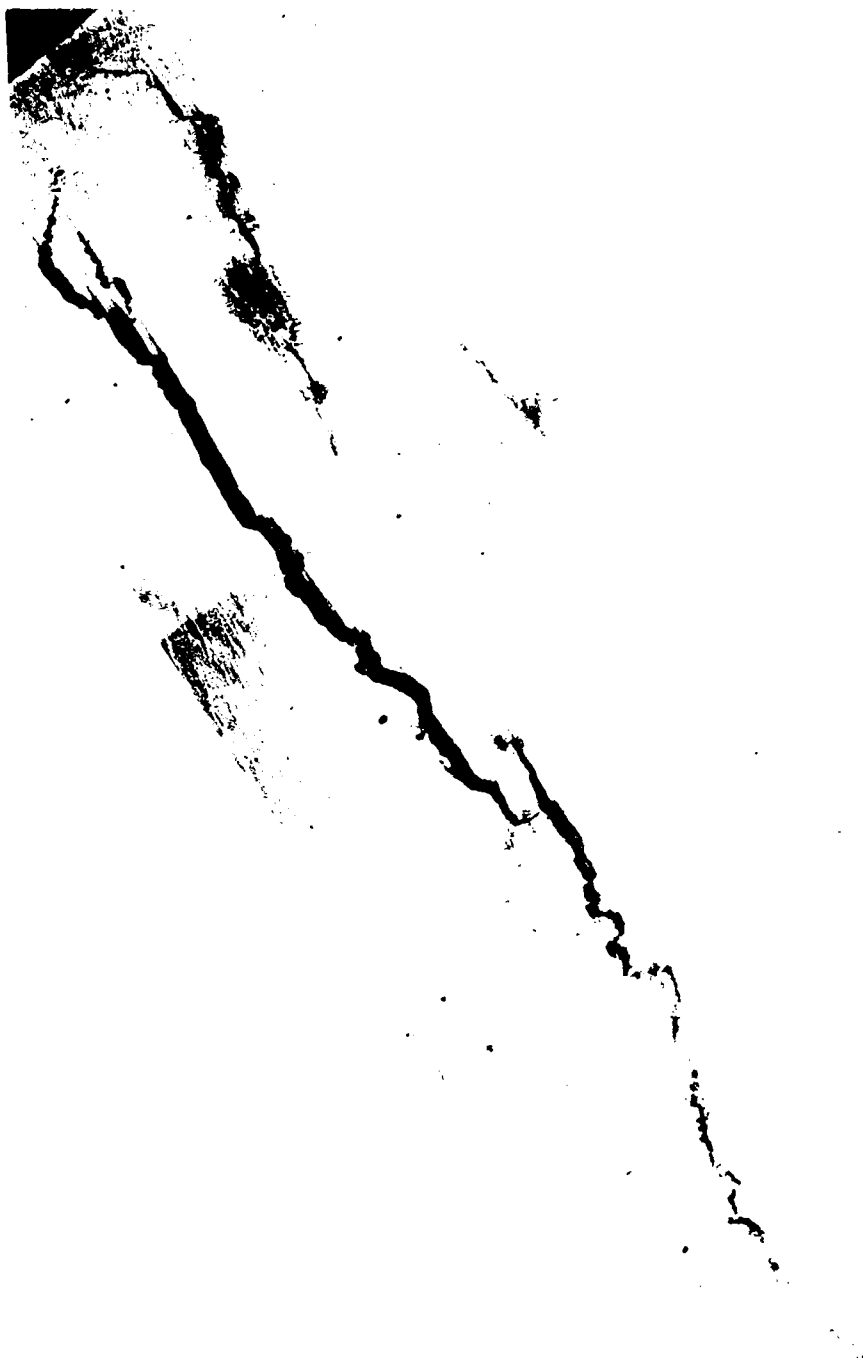


FIGURE 15 Typical Hydrogen-Assisted Crack. Sodium Bisulfite Etch Reveals Solidification Substructure, 40x.

with an X-Y recorder.

In welds with diffusible hydrogen content greater than 4 ppm, crack initiation and propagation occurred within a few minutes. In nearly all cases, cracking was not observed at all unless initiation occurred within ten minutes of loading.

Among specimens which cracked, most had acoustic-emission activity for many hours after loading. One ASC test showed crack growth for 33 hours after loading.

CONCLUSIONS

The conclusions drawn from this investigation of the hydrogen-assisted cracking of AX-140 welds on HY-130 steel and on AX-140 all-weld-metal specimens, utilizing the augmented strain cracking (ASC) test, are:

1. The pulsed-current gas metal arc welding (GMAW-P) process was found to be superior to the gas metal arc welding (GMAW) process for depositing weld metal containing predictable levels of diffusible hydrogen.
2. Both hydrogen and moisture additions to the shielding gas produced controlled diffusible hydrogen contents in weldments when the GMAW-P process was used. The use of moisture additions to the shielding gas produced welds with somewhat better arc characteristics than did the use of hydrogen additions.
3. For a given technique for adding hydrogen to the weld deposit, welds made with an energy input of 40 kJ/in. contained approximately the same diffusible hydrogen content as welds made with 30 kJ/in.
4. In HY-130 plate material, elongated inclusions, with long axes perpendicular to the stress produced by a plastic strain of 1.15%, served as initiation sites for cracking in the absence of hydrogen. This cracking, in the absence of hydrogen, did not occur when the long axes of the inclusions were parallel to the stress.

5. Although hydrogen-assisted cracking initiated solely in the fusion zone, cracking frequently propagated into the heat-affected zone.
6. Crack propagation through weld metal did not consistently follow the solidification structure.
7. The critical hydrogen content required to initiate cracking in AX-140 welds on HY-130 materials was approximately 1 ppm for an augmented strain of 1.15%. Increasing the augmented strain from 1.15% to 1.7% did not alter this critical hydrogen content appreciably.
8. An augmented strain of 0.55% was sufficient to initiate and propagate hydrogen-assisted cracks in HY-130 weldments when approximately 5 ppm diffusible hydrogen was present. A strain of 0.45% was equivalent, elastically, to a stress of 135,000 psi, the approximate yield strength of the AX-140 weld metal and the HY-130 base metal.
9. All-weld-metal ASC specimens, cut from four orientations with respect to the welding direction, had a susceptibility to hydrogen-assisted cracking which was less than that of test welds on HY-130 base-metal specimens. The critical hydrogen content required to initiate cracking at 1.15% augmented strain was approximately 3 ppm.
10. The critical hydrogen content of all-weld-metal specimens was not sensitive to orientation. However, when the ASC specimen was a transverse section of the all-weld-metal pad and the weld deposit was perpendicular

to the original welding direction, the critical hydrogen content for crack initiation was approximately 2 ppm.

11. The difference in susceptibility to hydrogen-assisted cracking between AX-140 welds on HY-130 plate and AX-140 welds on AX-140 all-weld-metal specimens has been ascribed to the difference in chemical composition of the fusion zones.

LITERATURE CITED

- 1) Sawhill, J.M, Dix, A.W., and Savage, W.F., "Modified Implant Test for Studying Delayed Cracking", Welding Journal, 53 (12), Res. Suppl. 554s-559s (1974).
- 2) Zapffe, C.A., and Sims, C.E., "Hydrogen Embrittlement Internal Stress and Defects in Steel", Trans. AIME, 145, 225-261 (1941).
- 3) Tetleman, A.S., Fracture of Solids, Wiley and Sons, New York (1962).
- 4) Petch, N.J. and Stables, P., "Delayed Fracture of Metals Under Static Load", Nature, 162, 842-843 (1952).
- 5) Williams, D.P., and Nelson, H.G., "Embrittlement of 4130 Steel by Low-pressure Gaseous Hydrogen", Met. Trans., 1 (1), 63-68 (1970).
- 6) Barth, C.F. and Steigerwald, E.A., "Evaluation of Hydrogen Embrittlement Mechanisms", Met. Trans., 1 (12), 3451-3455 (1970).
- 7) Troiano, A.R., "The Role of Hydrogen and Other Interstitials in the Mechanical Behavior of Metals", Trans. ASM, 52 (1), 54-80 (1960).
- 8) Oriani, A.R., "A Mechanistic Theory of Hydrogen Embrittlement of Steels", Hydrogen Damage, American Society for Metals, Metals Park, Ohio, 301-310 (1977).
- 9) Steinman, J.B., VaNess, H.C. and Ansell, G.S., "The Effect of High-Pressure Hydrogen upon the Notch Tensile Strength and Fracture Mode of 4140 Steel" Welding Journal, 54 (6), Res. Suppl. 221s-224s (1965).
- 10) Beachem, C.D., "A New Model for Hydrogen Assisted Cracking (Hydrogen Embrittlement)", Met. Trans., 3 (2), 437-451 (1972).
- 11) Savage, W.F., Nippes, E.F., and Silvia, A.J., "Prevention of Hydrogen-Induced Cracking in HY-130 Weldments". Interim Technical Report NR 031-78C 1977.
- 12) Savage, W.F., and Lundin, C.D., "The Vapour Strain Test" Welding Journal, 44 (10), Res. Suppl. 433s-443s (1965).

- 13) Savage, W.F., Nippes, E.F., and Pellman, M.A.,
"Hydrogen-Induced Cracking in Soviet Steels
Involved in USA/USSR Exchange Program," Welding
Journal, 55 (11), Res. Suppl., 315s-323s (1979).
- 14) Hartbower, C.E., Gerberich, W.W., and Crimmons, P.
P., "Monitoring Subcritical Crack Growth by De-
tection of Elastic Waves," Welding Journal, 47
(1), Res. Suppl., 1s-18s (1968).
- 15) Ball, D.J., Gestal, W.J., and Nippes, E.F.,
"Determination of Diffusible Hydrogen in Weldments
by the RPI Silicone-Oil Extraction Method," Welding
Journal, 60 (3) Res. Suppl., 50s-56s (1981).
- 16) Coe, F.R., "Hydrogen in Weld Metal," British Welding
Research Association Bulletin, Vol. 8 (1967).

3-8
DTIC